RSC Advances

ROYAL SOCIETY
OF CHEMISTRY

www.rsc.org/advances
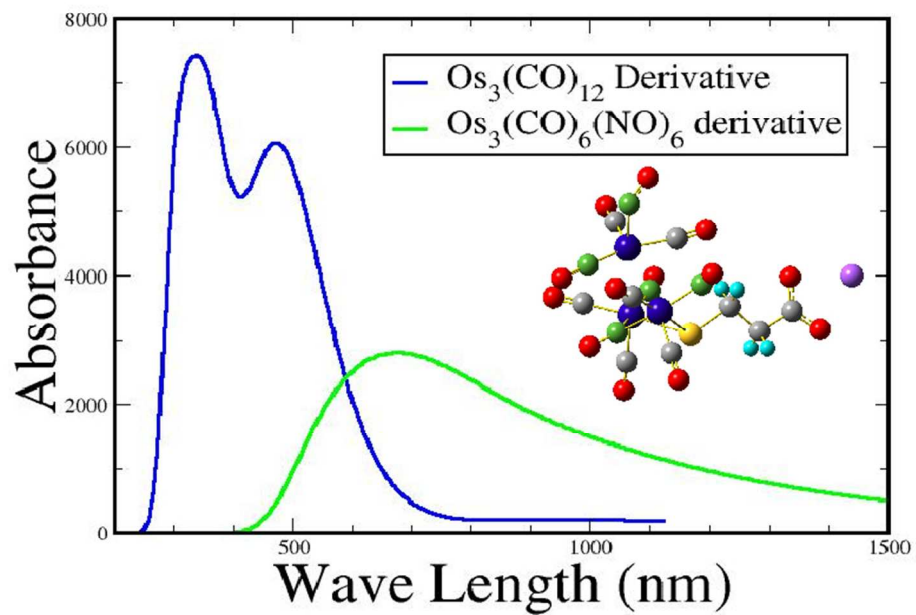
269x198mm (80 x 80 DPI)

Computational investigation of ligand field effect to improve photoacoustic contrast behavior of organometallic carbonyl clusters

Arijit Bag,[a] **Pradip Kr. Ghorai** [*a]

Water soluble organometallic carbonyl clusters are bio-compatible, stable and reliable high-contrast photoacoustic contrast agent (PACA). But they have limited application and efficacy due to their absorption in the visible region which has poor penetration depth inside tissue. In this article, we present the molecular level understanding of these compounds and investigate an alternative way to improve their PACA behavior. We discover that organometallic nitrosyl carbonyl compounds such as $[Os_3(CO)_6(NO)_4(\mu - NO)(\mu - S(CH_2)_2COO)]^- Na^+$ which shows high absorption at near infra-red region ($\lambda_{max} = 755nm$) is more suitable photoacoustic contrast agent than other carbonyl clusters which are reported in the literature till date. As metal nitrosyl bond is easily oxidisable, these compounds may also be used to study the reactive oxygen species in living cell. We introduce a theoretical model to calculate relative toxicity of a compound in terms of electric dipole moment (μ) and reactivity index (ω). Thus we compute μ and ω of all the clusters. It is shown that the modeled nitrosyl carbonyl compound is very less toxic than the reported carbonyl clusters.

1 Introduction

Photoacoustic spectroscopy[1,2] is one of the most important field of research today due to it's spatial resolution and deeper tissue penetration capability in live cell imaging.[3–8] Now a days exogenous contrast agents[9] are used for most of the cell imaging techniques.[7,8,10,11] For photoacoustic imaging, several classes of contrast agents have been tried among which organic dyes,[12,13] nanoparticles,[14–18] nanodyes[19] and organometallic cluster compounds[20] are main focus of interests. All these contrast agents have many advantages over the other and also have some drawbacks. Very recently organometallic cluster compounds, $M_3(CO)_{12}$ [where $M = Fe, Ru$ and Os] of group 8 elements have been used as PACA.[20] These compounds have drawn huge interests due to their bio-compatibility, solubility, stability and negligible cytotoxicity.[21–23] These compounds have also been used to synthesize effective anti$-$angiogenic agents which may be used for cancer treatment.[24] They are the common synthetic precursors to other organometallic complexes also.[25–27]

These compounds are surface active catalysts and have shown to catalyze the Fischer-Tropsch[28,29] and water-gas shift[30] reactions. But application of these compounds as PACA is limited due to their optical absorbance is at visible region.[20] Photoacoustic tomography is used for live cell imaging to detect live threatening deceases like cancer, tumor etc. This method has more accuracy than other imaging techniques say, MRI, CT scan, USG etc. A very good PACA should exhibit significant absorbance within 700 nm to 1000 nm as absorbance in this region by living cell is very less. In this

article we report the molecular level understanding of these compounds and discover new compounds which exhibit absorbance at longer wave length (λ) through effective ligand substitution.

2 Theory

The linearized photoacoustic energy equation[12,31] for a light absorptive material is defined as

$$\zeta\nabla^2\tau - \rho C\frac{\partial\tau}{\partial t} = -\mathscr{H}(t) - \frac{\rho C(\gamma-1)}{\beta}\frac{\partial\delta}{\partial t} \qquad (1)$$

where τ is a small perturbation in the temperature, $\zeta, \rho, C, \beta, \delta$ and γ are the thermal conductivity, density of the absorbent, heat capacity at constant volume, thermal expansivity, density perturbation and specific heat ratio respectively. $\mathscr{H}(t)$ is the amount of heat generated due to the photoacoustic interaction. Photoacoustic interaction in a material, when exposed to the light can be written as a function of absorption coefficient (μ_a) and time integrated flux density, fluence (Φ),[32] as follow

$$\mathscr{H}(x,t) = \mu_a(x)\Phi(x,t,\mu_a) \qquad (2)$$

where, x is the position vector and t is the absorption time. It is known that the optical penetration depth is inversely proportional to the absorption coefficient (μ_a) and hence proportional to the wave length λ of the incident radiation as follows[33]

$$\mu_a = \frac{4\pi k}{\lambda} \qquad (3)$$

where k is molar extinction co-efficient. From equation 2 and 3, we can say that a photoacoustic signal $\mathscr{H}(x,t)$ is inversely

[a] _Indian Institute of Science Education and Research Kolkata, Mohanpur-741246, West Bengal, India. E-mail:pradip@iiserkol.ac.in_

proposal to λ. If λ varies within the tissue transparent window of 700 nm to 1000 nm, a great contrast to the background signal is expected. Thus, for better contrast, one must use a radiation of longer λ. It is also possible to increase the signal strength by increasing the Φ [see equation 2] within the biomedical application limit.[34] By reducing the pulse duration (t_p), Φ can also be increased provided $t_p \ll \frac{4\pi k}{\lambda}$.[12] Thus, for compounds which have very small value of oscillator strength may also be used successfully as PACA by using high frequency laser pulse.

To calculate relative toxicity (γ), we use absolute hardness (η),[35] absolute electronegativity (χ) and reactivity index(ω) of a compound.[36,37] These three properties are calculated from the following relations

$$\eta = \frac{E_{LUMO} - E_{HOMO}}{2} \qquad (4)$$

$$\chi = -\frac{E_{LUMO} + E_{HOMO}}{2} \qquad (5)$$

$$\omega = \frac{\chi^2}{2 * \eta} \qquad (6)$$

where E_{HOMO} is the highest occupied molecular orbital energy and E_{LUMO} is the lowest unoccupied molecular orbital energy. Toxicity (C_{tox}) and reactivity index (ω) is related as follow[37]

$$C_{tox} = k_1 + k_2\omega \qquad (7)$$

where k_1 and k_2 are the constants. For large value of ω, $\frac{k_1}{k_2} \ll \omega$ and hence

$$C_{tox} \propto \omega \qquad (8)$$

Toxicity also depends on the partition co-efficient ($P_{o/w}$) of the compound in 1-octanol and water. Considering Deneer's equation[38] we get toxicity is related to $P_{o/w}$ as follows

$$C_{tox} \propto (P_{o/w})^{-0.36} \qquad (9)$$

Thus, we can write

$$C_{tox} \propto \omega(P_{o/w})^{-0.36} \qquad (10)$$

Bayat and Movaffagh[39] showed that partition co-efficient may be expressed in terms of solvation free energy of the compound in two different solvents as below

$$P_{o/w} = \frac{e^{\frac{\Delta G_{sol,w}}{RT}}}{e^{\frac{\Delta G_{sol,oct}}{RT}}} \qquad (11)$$

where, $\Delta G_{sol,w}$ and $\Delta G_{sol,oct}$ are the solvation free energies of the compound in water and in 1-octanol, T is the temperature and R is the universal gas constant. Solvation free energy in water is the measure of dipole-dipole interaction between the

solute and solvent. Thus, we may consider that $\Delta G_{sol,w}$ is proportional to the dipole moment (μ) of the solute *i.e.* dipole moment of the compound. If test compound and reference compound are of the same type then $\Delta G_{sol,oct}$ is constant. we may consider $P_{o/w} \propto e^{k\mu}$ where k is the constant for a particular temperature. Using equation 10, we get

$$C_{tox} \propto \omega e^{-k\mu} \qquad (12)$$

Now if we define the subscripts *ref* and *comp* for the reference compound and the compound under investigation respectively then, γ of similar compounds can be written as

$$\begin{aligned} \gamma &= \frac{(C_{tox})_{comp}}{(C_{tox})_{ref}} \\ &= \frac{\omega_{comp}e^{k\mu_{ref}}}{\omega_{ref}e^{k\mu_{comp}}} \\ &= \frac{\frac{\omega_{comp}}{\omega_{ref}}}{e^{k(\mu_{comp}-\mu_{ref})}} \end{aligned} \qquad (13)$$

k may also be considered as a scaling factor. For simplicity, we assume $k = 1$. Hence, relative toxicity of similar compounds is as below

$$\gamma = \frac{\frac{\omega_{comp}}{\omega_{ref}}}{e^{(\mu_{comp}-\mu_{ref})}} \qquad (14)$$

Thus, γ_{ref} is 1.0. If γ of a compound is greater than 1.0, compound is more toxic than the reference one.

3 Computational Details

All the calculations are performed by using Gaussian 09 package.[40] The structures are optimized without any symmetry constraints. All the minimum energy structures are confirmed by the harmonic vibrational frequency without any imaginary mode. The convergence thresholds are set to 0.000015 Hartree/Bohr for the forces, 0.00006 Å for the displacement and 10^6 Hartree for the energy change. All calculations are performed with the density functional theory (DFT) with unrestricted Beckes three parameter hybrid exchange functional[41] combined with Lee−Yang−Parr non-local correlation function[42], abbreviated as B3LYP. We have used LanL2DZ basis set[43,44] along with the corresponding Los Alamos relativistic effective core potentials[45] provided by Gaussian 09 package. We have performed time dependent density functional theory (TDDFT) calculation for UV-visible spectra of the chosen compounds. It is reported that, for large main group element clusters B3LYP/LanL2DZ method is sufficient.[46–51]
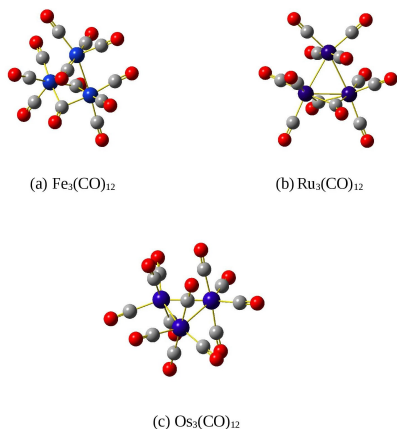
(a) Fe₃(CO)₁₂

(b) Ru₃(CO)₁₂

(c) Os₃(CO)₁₂

Fig. 1 Optimized geometries of $M_3(CO)_{12}$ $(M = Fe, Ru$ and $Os)$ metal carbonyl clusters

Fig. 2 UV-Visible spectra of different $[M_3(CO)_{12}$ clusters, where $M = Os, Ru$ and $Fe]$

4   Results and Discussion

4.1   Metal Carbonyl Clusters

First we perform geometry optimization of the three trimetal carbonyl clusters, $Fe_3(CO)_{12}$, $Ru_3(CO)_{12}$ and $Os_3(CO)_{12}$ in gas phase. Figure 1 represents the optimized structures and Table 1 lists the metal - metal $(M - M)$ bond distances of these carbonyl clusters. In Fe cluster, two metal atoms are connected through two bridging CO. Bond distance between the two Fe atoms is 2.59 Å which is very close with the experimental value of 2.57 Å. Two other metal-metal bonds, i.e. bonds between bridging and non-bridging metals are 2.68 Å as compared to the experimental value of 2.70 Å. In case of Ru cluster, bond between bridging atoms are 2.86 Å which is again in agreement with the experimental value of 2.85 Å. The bonds between the bridging and non-bridging metals are 2.89 Å as compared to the experimental value of 2.85 Å and 2.86 Å. For both Fe and Ru clusters, bonds between bridging and non-bridging metals are larger than the bridging $M - M$ bond distance which is expected because bridging stabilises the bond. On the other hand, in case of Os cluster, all three metal-metal bonds are nearly same and there is no bridging carbonyl. The $M - M$ bond distances are 2.89 Å, 2.89 Å and 2.89 Å which are in very good agreement with the experimental values of 2.87 Å, 2.88 Å and 2.88 Å respectively.

By using these optimized structures, we compute the absorption spectra for all the three clusters. Calculated values of the absorption peaks which are listed in Table 1 are in very good agreement with the experiment. Only for Fe cluster, computed value at 565 nm has a deviation of 37 nm from the experimental value else deviation is less than 10 nm. In Osmium cluster, we find all three absorption peaks are in fact a result of overlapping of two near degenerate transitions which
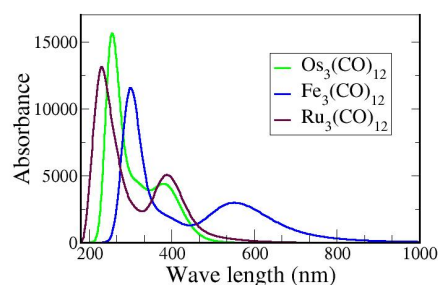
are probably due to the higher order of symmetry. Thus for Osmium cluster, absorbance intensity is higher than Fe and Ru clusters. A comparative absorption spectra is presented in Figure 2. Nature of all the three plots are similar, only their absorption peaks are at different frequency.

4.2   Metal Carbonyl Cluster Derivatives

(a) Fe₃(CO)₁₂ derivative

(b) Ru₃(CO)₁₂ derivative

(c) Os₃(CO)₁₂ derivative
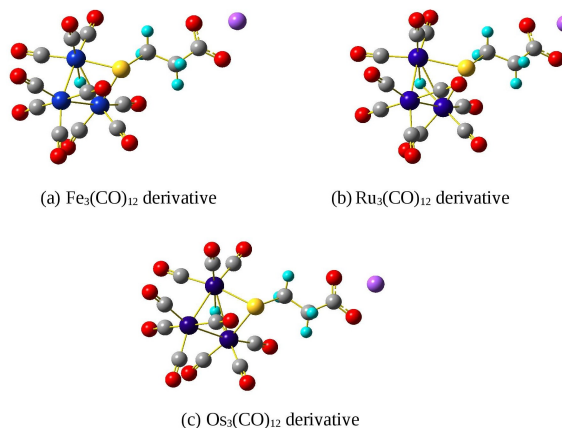
Fig. 3 Optimized geometries of metal carbonyl cluster derivatives

From the metal carbonyl cluster studies it is not clear why Osmium cluster has better contrast as PACA.[20] Thus, we compute the UV-visible absorption spectra of all carbonyl cluster derivatives to justify the experimental results reported by Kong $et.$ $al.$[20] Figure 3 represents three optimized geometries of carbonyl cluster derivatives of Fe, Ru and Os. We use thio-acetate derivative of the Fe, Ru and Os clusters $[M_3(CO)_{10}(\mu - H)(\mu - S(CH_2)_2COO^-)Na^+]$ as the experiment was done by Kong $et.$ $al.$ with this derivative. Optimized structures are shown in Figure 3. Due to organic ligand

Table 1 Absorption maxima and other properties of $Fe_3(CO)_{12}$, $Ru_3(CO)_{12}$ and $Os_3(CO)_{12}$ clusters

Compound	Calculated absorbance peak (nm)	Experimental[52,53] absorbance peak (nm)	$M-M$ bond distance (Å) (calculated)	$M-M$ bond distance (Å) (experimental)	Charge on metal (au)
$Fe_3(CO)_{12}$	565	602[52]	2.59 ^{b}	2.57$^{b\,55}$	-0.940^b
	301	310[52]	2.68	2.70	-0.940^b
			2.68	2.70	-0.653
$Ru_3(CO)_{12}$	390	390[52] 392[53]	2.86 ^{b}	2.85[56]	0.059^b
	230	238[52]	2.89	2.85	0.059^b
			2.89	2.86	0.216
$Os_3(CO)_{12}$	386.71, 386.55	385[52,53]	2.89	2.87[56]	0.171
	320.93,320.87	330[52,53]	2.89	2.88	0.171
	254.43,254.43	240[52,54]	2.89	2.88	0.171

^{b} indicates metal atoms (or bond between two atoms) which are connected by bridging ligand.

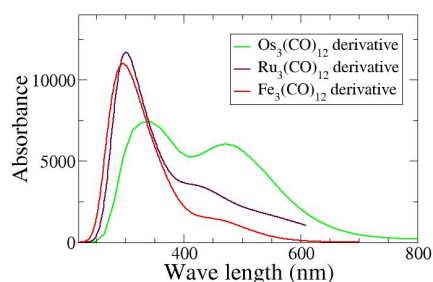substitution geometries of all three clusters have significantly changed.

Fig. 4 UV-Visible spectra of different metal carbonyl cluster derivatives $[M_3(CO)_{10}(\mu-H)(\mu-S(CH_2)_2COO^-)Na^+$, where $M = Os, Ru$ and Fe]

From Table 2 it is seen that both in Fe and Ru clusters metal-metal bond between two bridged metal increases by 0.07 Å but bond between bridging and non-bridging metals remains almost same as the deviation is less than 0.01 Å. A dramatic change is observed for Osmium cluster. Here symmetry is lost. Sulfide and hydride ions act as metal-ligand-metal $(M-L-M)$ bridging. As a result, bond between two bridging Os is decreased by 0.29 Å and two other bonds are decreased by 0.21 Å and 0.20 Å respectively. Figure 4 represents the UV-visible spectra of these compounds. The absorption peak of Fe and Ru derivatives have a blue shift, where as Os derivative shows red shift. From Table 2, it is clear from the maximum value of the absorption peak that Os derivative is better PACA than Fe and Ru derivatives. The significant change in UV-visible spectra is due to their different structural transformation which is observed due to organic ligand substitution. In the cluster only form *i.e.* in $M_3(CO)_{12}$, we observe

two bridging CO ($M-L-M$ bridge) for both Fe and Ru but not for Os. Interestingly, in derivatives form, Os cluster also shows $M-L-M$ structure like Fe and Ru. Thus, the red shift of Os derivative is only due to the change of geometry. We also observe that for Fe and Ru derivatives, only one absorption peak is obtained instead of two for unsubstituted carbonyl clusters. For Os, there are two peaks, but they become broad.

Charge density analysis (see Table $-$ 1) shows that in the cluster only form, all Fe atoms are negatively charged, Ru atoms have very small positive charge where as Os atoms are positively charged. In Fe and Ru clusters, bridging atoms are more negative or less positive than non-bridging atom and bond distance between the $M-M$ bridging atoms is less than the non-bridging bonds. This implies that due to bridging, ligand to metal charge transfer occurs. In the Os cluster, all three metals have same positive charge which indicates the absence of ligand to metal charge transfer. Due to more positive charge on Os and larger value of crystal field splitting energy, it is more stable than Fe and Ru cluster.

For the Os cluster, recent experiment did not observe any significant difference in absorbance due to salt derivative formation. We observe one absorption peak at 386 nm with oscillator strength 0.05 for the pure cluster whereas for the derivative [see Figure 4] there are two distinct peaks of nearly equal intensities, one is at 475 nm with oscillator strength 0.06 and another is at 340 nm with oscillator strength 0.08. Thus, due to salt formation and hence change of ligand field, optical property of the compound changes significantly. If we consider the overlap between the two absorption maxima, we find a maximum at 407.5 nm which is very good agreement with the experimental observed value of 410 nm.[20]

Analyzing the excited states of $M_3(CO)_{12}$ clusters and their derivatives, we observe degeneracy only for lowest unoccupied molecular orbital (LUMO) of $Os_3(CO)_{12}$ cluster which does not contain any bridging atom. But due to bridging in the derivative form, the degeneracy is lost. The loss of degeneracy

Table 2 Absorption maxima of $Fe_3(CO)_{12}$, $Ru_3(CO)_{12}$ and $Os_3(CO)_{12}$ cluster derivatives.

Compound	Calculated absorbance peak (in nm)	Oscillator strength (calculated)	Homo-Lumo energy gap(au)	M-M bond distance (Å) (calculated)	Charge on metal (au)
$Fe_3(CO)_{12}$ derivative	300	0.14	0.12101	$2.66^{\,b}$	-0.856^b
				2.69	-0.855^b
				2.69	-0.782
$Ru_3(CO)_{12}$ derivative	296	0.045	0.12975	$2.92^{\,b}$	-0.094^b
				2.88	-0.093^b
				2.88	0.190
$Os_3(CO)_{12}$ derivative	473	0.060	0.05965	$2.61^{\,b}$	0.132^b
	349	0.075		2.70	0.180^b
				2.69	0.725

^{b} indicates metal atoms (or bond between two atoms) which are connected by ligand bridge.

is responsible for the decreases of absorbance. These twofold degeneracy indicates electronic transition from one metal to two other equivalent metal centers. But due to presence of ligand in the bridge, two metal atoms differs from the rest. In that situation the absence of degeneracy indicates that the electron transition occurs from bridging metals to non-bridging metal.

4.3 Effect of Organic Chain Length

To model improved PACA using this compound, first we change the organic chain length keeping functional group fixed. From Table 3, we find that for $C = 3$ [C is the number of carbon atom present in the organic salt] PAC activity is the maximum. From the charge distribution of the residue, we find that for $C = 3$, charge on the S atom is maximum [-0.286] and very large as compared to $C = 2, 4$ and 5. Same charge on S for $C = 2, 4$ and 5 yields same position of the absorption maxima of the corresponding derivatives irrespective of the salt.

Table 3 Dependence of organic chain length on optical absorption of $Os_3(CO)_{12}$ derivative.

Number of carbon atoms in the residue	Charge on sulfur atom	Lowest energy absorption peak (nm)	Oscillator strength (calculated)
2	-0.069	290	0.05
3	-0.286	475	0.06
4	-0.072	287	0.07
5	-0.070	294	0.07

4.4 Effect of NO Substitution

As we do not observe significant improvement in the PACA by substituting the organic chain, we substitute strong field CO ligand by a weak field NO ligand. For the Osmium nitrosyl carbonyl cluster, such as $Os_3(CO)_{10}(NO)_2$ we find the existence of bridging NO which agrees very well with the experiment.[57] As discussed before, we do not observe any bridging CO for $Os_3(CO)_{12}$ cluster. The different metal$-$ligand bonding is due to the crystal field splitting. In presence of strong field CO ligand, crystal field splitting stabilization energy is high and hence strong metal$-$metal bond formation is favorable. Thus, only terminal metal$-$ligand binding occurs in case of $Os_3(CO)_{12}$ cluster. Appearance of a weak field ligand weaken the $M-M$ bond and leads to the formation of $M-L-M$ bridge. Metal$-$metal bond analysis of two optimized geometries, $Os_3(CO)_{12}$ and $Os_3(CO)_{10}(NO)_2$ support this argument. All $M-M$ bond distances in $Os_3(CO)_{12}$ are 2.89 Å, whereas in $Os_3(CO)_{10}(NO)_2$ the bond distances are 2.96, 2.96 and 3.26 Å. It is seen that one $Os-Os$ bond where two bridging ligands are connected, is elongated maximum as a reflection of weak $M-M$ bonding. This change of geometry and ligand field around the metals also cause red-shift[54] and blue-shift [from 386 $nm \rightarrow$ 339 nm] in UV-visible spectrum. The metal$-$metal bond distances in $Os_3(CO)_{11}(NO)$ cluster are 2.88, 2.90 and 2.90 Å. Though due to substitution of one CO by one NO does not affect the metal-metal bond length significantly, a huge red-shift in UV-Visible spectra [386 $nm \rightarrow$ 494 nm, change is 108 nm] is observed. Due to one NO substitution, HOMO-LUMO energy gap decreases from 0.14336 au to 0.10673 au $i.e.$ by 109 nm which is exactly same as the spectral shift of 108 nm. Thus, the spectral shift is only due to the change of ligand field. For this compound the lowest energy transition is a metal$-$metal $d-d$ transition. Thus, for osmium cluster derivative, to improve PAC behavior we have to substitute CO by a weak field ligand.

Following this, we compute the lower energy absorption spectra of all possible osmium nitrosyl carbonyl compounds. Interestingly, there is no linear dependence of λ_{max} [wave length for maximum absorbance] with the number of NO. We

Table 4 Absorption peak of $Os_3(CO)_{12}$ cluster due to substitution of CO by NO ligand

Composition	Absorbance peak (in nm)	Oscillator strength
$Os_3(CO)_{12}$	386	0.091
$Os_3(CO)_{11}(NO)$	494	0.046
$Os_3(CO)_{10}(NO)_2$	339	0.025
$Os_3(CO)_9(NO)_3$	361	0.014
$Os_3(CO)_8(NO)_4$	337	0.028
$Os_3(CO)_7(NO)_5$	429	0.006
$Os_3(CO)_6(NO)_6$	654	0.028
$Os_3(CO)_5(NO)_7$	545	0.006
$Os_3(CO)_4(NO)_8$	540	0.034
$Os_3(CO)_3(NO)_9$	674	0.006
$Os_3(CO)_2(NO)_{10}$	655	0.016
$Os_3(CO)_1(NO)_{11}$	764	0.004
$Os_3(NO)_{12}$	939	0.005

discover that though $Os_3(NO)_{12}$ compound has the highest λ_{max} of 939 nm (see Table 4), it's oscillator strength is very low (0.006). Thus, Considering both high value of λ_{max} and acceptable value of oscillator strength, $Os_3(CO)_6(NO)_6$ may be the best PACA [$\lambda_{max} = 657$ nm and oscillator strength is 0.03]. Same organic salt substitution to this compound leads to a better PACA [$\lambda_{max} = 755$ nm and oscillator strength is 0.0134].
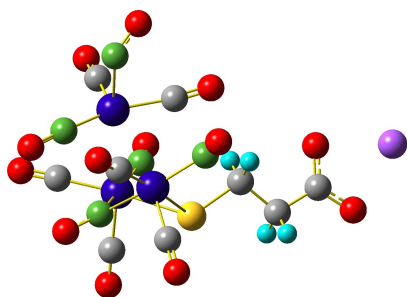
Fig. 5 Optimized structure of $Os_3(CO)_6(NO)_4(\mu - NO)(\mu - S(CH_2)_2COO^-)Na^+$

Since we have found that $Os_3(CO)_6(NO)_4(\mu - NO)(\mu - S(CH_2)_2COO^-)Na^+$ compound may be the best PACA, we further study this compound extensively. To find the solvent effect on this compound, we include water as a solvent. For this particular study we use IEFPCM model and B3PW91 functional with the same basis set. Optimized structure is given in Figure 5. Metal-metal bond distances are 3.22 Å for bridging metals and 3.06 Å and 2.97 Å for bridging to non-bridging metal.

IR and UV-visible spectra of $Os_3(CO)_6(NO)_4(\mu - NO)(\mu - S(CH_2)_2COO^-)Na^+$ are shown in Figure 6 and Figure 7 respectively. It is observed that our modeled compound
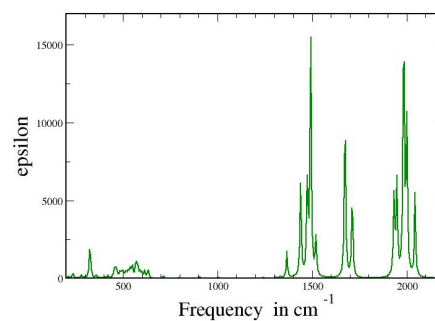
Fig. 6 IR spectra of $Os_3(CO)_6(NO)_4(\mu - NO)(\mu - S(CH_2)_2COO^-)Na^+$
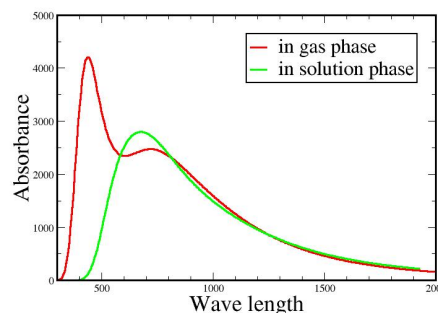
Fig. 7 UV-visible spectra of $Os_3(CO)_6(NO)_4(\mu - NO)(\mu - S(CH_2)_2COO^-)Na^+$

shows similar efficiency as PACA in solution phase also. Absorption above 800 nm is same for both gas phase and solution phase. within 500 nm to 800 nm, solution phase has better efficiency. Thus, use of this compound as PACA is viable. We find that it is a very strong polar compound with dipole moment 14.29 Debye. Thus, it is expected that this compound would be highly water soluble and hence less cytotoxic. Comparison of relative toxicities of three cluster derivatives and this nitro- substituted compound are presented in Table 5. Osmium carbonyl cluster is taken as the reference compound. We know that cytotoxicity depends on reactivity index and $logP_{o/w}$[58,59]. As discussed before, a compound of high dipole moment(μ) should have low value of $logP_{o/w}$ and low toxicity.[58] On the other hand, high value of reactivity index (ω) is corresponds to high toxicity. Here we compute the relative toxicity as mentioned in the theory section. In this parameter we find that $Ru_3(CO)_6(NO)_4(\mu - NO)(\mu - S(CH_2)_2COO^-)Na^+$ compound has six times (6.227) higher toxicity than $Os_3(CO)_{10}(\mu - H)(\mu - S(CH_2)_2COO^-)Na^+$. Our modeled compound, $Os_3(CO)_6(NO)_4(\mu - NO)(\mu -$

Table 5 Reactivity descriptors and relative toxicity (with respect to Osmium cluster derivatives) of three metal carbonyl cluster derivatives and our modeled compound

Compounds	Absolute hardness (η)	Absolute electro-negativity (χ)	Reactivity index (ω)	Dipole moment (μ)	Relative toxicity (γ)
$Fe_3(CO)_{10}$salt	0.060	0.1779	0.2628	11.954	0.014
$Ru_3(CO)_{10}$salt	0.050	0.1760	0.3094	5.988	6.227
$Os_3(CO)_{10}$salt	0.071	0.1753	0.2161	7.458	1.00
$Os_3(CO)_6(NO)_5$salt	0.024	0.1876	0.7325	14.292	0.004

$S(CH_2)_2COO^-)Na^+$, is extremely less toxic than osmium and iron cluster derivatives.

4.5 Free Energy (ΔG) Calculation for NO Substitution

Table 6 Calculation of free energy change for the substitution reaction of CO by NO ligand to $Os_3(CO)_{12}$

Composition	Free energy change(ΔG) (in a.u.) from previous derivative	Free energy change(ΔG) (in a.u.) from initial compound
$Os_3(CO)_{11}(NO)$	-0.3742	-0.3742
$Os_3(CO)_{10}(NO)_2$	-0.0463	-0.4205
$Os_3(CO)_9(NO)_3$	0.4498	0.0293
$Os_3(CO)_8(NO)_4$	-0.3892	-0.3599
$Os_3(CO)_7(NO)_5$	0.4405	0.0806
$Os_3(CO)_6(NO)_6$	-0.3738	-0.2932
$Os_3(CO)_5(NO)_7$	0.0038	-0.2894
$Os_3(CO)_4(NO)_8$	-0.4471	-0.7365
$Os_3(CO)_3(NO)_9$	0.0035	-0.7329
$Os_3(CO)_2(NO)_{10}$	0.0835	-0.6495
$Os_3(CO)_1(NO)_{11}$	-0.0002	-0.6497
$Os_3(NO)_{12}$	0.0169	-0.6328

We have modeled to improve PACA by substituting CO by NO ligand. Synthesis of these compounds may not be trivial. So far, mono- and di- substituted compounds have already been synthesized. Thus, using free energy calculation, we find out whether other substitutions are possible or not. Computed ΔG is listed in Table 6. ΔG for the first two substitutions [*i.e.* for $Os_3(CO)_{11}(NO)$ and $Os_3(CO)_{10}(NO)_2$] are negative. But overall free energy change for tri- substituted derivative is positive, same as penta- substituted derivative. Total free energy change for other derivatives are negative. From this calculation we conclude that tri- and penta- substituted derivative may not be prepared but rest can be prepared.

4.6 Drug Potentiality

As organometallic compounds are used as potential drug for several fatal diseases[24,60], we have tested our modeled compound, $Os_3(CO)_6(NO)_4(\mu - NO)(\mu - S(CH_2)_2COO^-)Na^+$, for few selective diseases using chemosophia in-silico test program[61]. This compound is found to have drug potentiality for AIDS, cancer and pain killer. Results of biological activity tests are given in Table- 7. It is also found as less eco-toxic. This supports our relative toxicity calculation result of this compound discussed earlier. CYP450-2D6 and CYP450-3A4 metabolism is possible for this compound.

Table 7 Drug potentiality of our modeled compound: an in-silico test using chemosophia[61] package

Biological activity	Success probability (%)
HIV1-proteaze inhibitory activity	**66.8**
Anti-Inflammatory activity (ks2-p38-MAP-kinase inhibitors)	**69.4**
Anti-Oxidant activity	33.8
Anti-Tumor Anti-mitotic activity	27.5
Anti-Tumor Dihydrofolate reductase inhibitory activity	25.9
Anti-Tumor Topoisomerase-II inhibitory activity	**99.6**
Eco-toxicity	8.7
Metabolism at CYP450-2D6	54.9
Metabolism at CYP450-3A4	78.9

5   Conclusions

We study UV-visible spectra of the organometallic carbonyl clusters as very recently these compounds are used as photoacoustic contrast agent. We find that $Os_3(CO)_6(NO)_4(\mu - NO)(\mu - S(CH_2)_2COO^-)Na^+$ is a better PACA with high absorption within 500 nm to 1000 nm. Absorption of this compound even extended up to 2000 nm. Thus, it may be used in IR detector. This compound is paramagnetic, hence it may be used as MRI contrast agent also. Absolute hardness(η) of this compound is 0.024 and reactivity(ω) is 0.7325 which suggest that it may be used to study reactive oxygen species in living cell. Free energy calculation shows that this compound can be easily synthesized. In-silico activity test of this compound shows very good activity to words HIV (66.8%) and cancer (99.6%). Other biological activities are given in Table- 7. From these study we can say that our modeled compound $Os_3(CO)_6(NO)_4(\mu - NO)(\mu - S(CH_2)_2COO^-)Na^+$ may serve as eco-friendly (as eco-toxicity is only 8.7%), biocompatible (as non-cytotoxic), water soluble deeper tissue penetrative (absorption at 700 nm to 1000 nm) PACA as well as effective drug for HIV, cancer and inflammation.

6   Acknowledgments

References

1 A. G. Bell, *Am. J. Sci.*, 1880, **20**, 305-324.

2 A. C. Tam, *Rev. Mod. Phys.*, 1986, **58**, 381-431.

3 L. V. Wang, *Med. Phys.*, 2008, **35**, 5758-5767.

4 N. V. Thakor, *J. Cereb. Blood Flow Metab.*, 2012, **32**, 936-937.

5 X. Wang, Y. Pang, G. Ku, X. Xie, G. Stocia and L. V. Wang, *Nat. Biotechnol*, 2003, **21**, 803-806.

6 X. Wang, Y. Pang, G. Ku, G. Stocia and L. V. Wang, *Opt. Lett*, 2003, **28**, 1739-1741.

7 D. J. Stephens and V. J. Allan, *Science*, 2003, **300**, 82-86.

8 J. K. Jaiswal, E. R. Goldman, H. Mattoussi and S. M. Simon, *Nature Methods*, 2004, **1**, 73-78.

9 V. Tsytsarev, C. Bernardelli and K. I. Maslov, *J. Neurosci. Neuroeng.*, 2012, **1**, 180-192.

10 R. B. Sekar and A. Periasamy, *The J. Cell Bio.*, 2003, **160**(5), 629-633.

11 X. Michalet, F. F. Pinaud, L. A. Bentolila, J. M. Tsay, S. Doose, J. J. Li, G. Sundaresan, A. M. Wu, S. S. Gambhir and S. Weiss, *Science*, 2005, **307**, 538-544.

12 K. Firouzi, E. Stride and N. Saffari, *J. Acoust. Soc. Am.*, 2013 **133**(6), 3853-3862.

13 A. Hellebust and R. Richards-Kortum, *Nanomedicine (London)*, 2012, **7**(3), 429-445.

14 A. Agarwal, S. W. Huang, M. OD́onnell, K. C. Dey, M. Dey, N. Kotov and S. Ashkenazi, *Appl. Phys. Lett.*, 2007, **102**, 064107 - 064107-4.

15 K. Pu, A. J. Shuhendler, J. V. Jokerst, J. Mei, S. S. Gambhir, Z. Bao and J. Rao, *Nature nanotech.*, 2014, **9**, 233-239; J. V. Jokerst, A. J. Cole, D. V. de Sompel and S. S. Gambhir, *ACS Nano*, 2012, **6**, 10366-10377.

16 Y. S. Chen, W. Frey, S. Kim, P. Kruizinga, K. Homan and S. Emelianov, *Nano Lett.*, 2011, **11**, 348-354.

17 M. Pramanik, M. Swierczewska, D. Green, B. Sitharaman and L. V. Wang, *J. Biomed. Opt.*, 2009, **14**, 034018 - 034018-8.

18 X. Liang, Z. Deng, L. Jing, X. Li, Z. Dai, C. Li and M. Huang, *Chem. Commun.*, 2013, **49**, 11029-11031.

19 C. J. Flynn, E. B. E. Oh, S. M. McCullough, R. W. Call, C. L. Donley, R. Lopez and J. F. Cahoon, *J. Phys. Chem. C*, 2014, **118**, 14177-14184.

20 K. V. Kong, Lun-De Liao, Z. Lam, N. V. Thakor, W. K. Leong and M. Olivo, *Chem. Commun.*, 2014, **50**, 2601-2603.

21 K. V. Kong, W. K. Leong and L. H. Lim, *Chem. Res. Toxicol.*, 2009, **22**, 1116-1122.

22 K. V. Kong, W. K. Leong, S. P. Ng, T. H. Nguyen and L. H. Lim, *Chem. Med. Chem.*, 2008, **3**, 1269-1275.

23 K. V. Kong, W. Chew, L. H. K. Lim, W. Y. Fan and W. K. Leong, *Bioconjugate Chem.*, 2007, **18**, 1370-1374.

24 A. A. Nazarov, M. Baquie, P. N. Sliwinska, O. Zava, J. R. van Beijnum, M. Groessl, D. M. Chisholm, Z. Ahmadi, J. S. McIndoe, A. W. Griffion, H. van den Bergh and P. J. Dyson, *Scientific Report*, 2013, **3**, 1485 - 1485-7.

25 M. G. Richmond, *Coord. Chem. Rev.*, 2004, **248**, 881-901.

26 N. E. Leadbeater, *J. Organomet. Chem.*, 1999, **573**, 211-216.

27 Y. M. Wuu, J. G. Bentsen, C. G. Brinkley and M. S. Wrighton, *Inorg. Chem.*, 1987, **26**, 530-540.

28 M. Deeba and B. C. Gates, *J. Catal.*, 1981, **67**, 303-307.

29 F. Hugues, A. Dalmon, P. Bussiere, A. K. Smith, M. J. Basset and D. Olivier, *J. Phys. Chem.*, 1982, **86**, 5136-5144.

30 R. Ganzerla, M. Lenarda, F. Pinna and M. Graziani, *J. Organomet. Chem.*, 1981, **208**, C43-C45.

31 H. X. Chen, I. E. McGrath, A. C. Beveridge and G. J. Diebold, *Proc. IEEE Ultrason. Symp.*, 1997, **1**, 719-725.

32 B. T. Cox P. C. Beard, *J. Acoust. Soc. Am.*, 2005, **117**, 3616-3627.

33 http://pveducation.org/pvcdrom/pn-junction/absorption-coefficient

34 M. Xu and L. V. Wang, *Rev. Sci. Instrum.*, 2006, **77**, 041101 - 041101-22.

35 R. G. Parr and R. G. Pearson, *J. Am. Chem. Soc.*, 1983, **105**, 7512-7516.

36 M. Ishihara, M. Kawase, G. Westman, K. Samuelsson, N. Motohashi and H. Sakagami, *Anticancer Research*, 2007, **27**, 4053-4058.

37 J. Padmanabhan, R. Parthasarathi, V. Subramanian and P. K. Chattaraj, *J. Phys. Chem. A*, 2006, **110**, 2739-2745.

38 J. W. Deneer, W. Sinnige and J. L. M. Hermens, *Aquatic Toxicology*, 1988, **12**, 185-192.

39 Z. Bayat and J. Movaffagh, *Russian J. Phys. Chem. A*, 2010, **84**, 2293-2299.

40 Gaussian 09, Revision D.01, M. J. Frisch, G. W. Trucks, H. B. Schlegel, G. E. Scuseria, M. A. Robb, J. R. Cheeseman, G. Scalmani, V. Barone, B. Mennucci, G. A. Petersson, H. Nakatsuji, M. Caricato, X. Li, H. P. Hratchian, A. F. Izmaylov, J. Bloino, G. Zheng, J. L. Sonnenberg, M. Hada, M. Ehara, K. Toyota, R. Fukuda, J. Hasegawa, M. Ishida, T. Nakajima, Y. Honda, O. Kitao, H. Nakai, T. Vreven, J. A. Montgomery, Jr., J. E. Peralta, F. Ogliaro, M. Bearpark, J. J. Heyd, E. Brothers, K. N. Kudin, V. N. Staroverov, R. Kobayashi, J. Normand, K. Raghavachari, A. Rendell, J. C. Burant, S. S. Iyengar, J. Tomasi, M. Cossi, N. Rega, J. M. Millam, M. Klene, J. E. Knox, J. B. Cross, V. Bakken, C.

Adamo, J. Jaramillo, R. Gomperts, R. E. Stratmann, O. Yazyev, A. J. Austin, R. Cammi, C. Pomelli, J. W. Ochterski, R. L. Martin, K. Morokuma, V. G. Zakrzewski, G. A. Voth, P. Salvador, J. J. Dannenberg, S. Dapprich, A. D. Daniels, . Farkas, J. B. Foresman, J. V. Ortiz, J. Cioslowski, and D. J. Fox, *Gaussian, Inc.*, Wallingford CT, 2009.

41 A. D. Becke, *Phys. Rev. A*, 1988, **38**, 3098-3100.

42 C. Lee, W. Yang and R. G. Parr, *Phys. Rev. B*, 1988, **37**, 785-789.

43 P. J. Hay and W. R. Wadt, *J. Chem. Phys.*, 1985, **82**, 270-283.

44 W. R. Wadt and P. J. Hay, *J. Chem. Phys.*, 1985, **82**, 284-298.

45 P. J. Hay and W. R. Wadt, *J. Chem. Phys.*,1985, **82**, 299-310.

46 S. Chiodo, N. Russo and E. Sicilia, *J. Chem. Phys.*, 2006, **125**, 104107 - 104107-8.

47 J. F. Alvino, T. Bennett, D. Anderson, B. Donoeva, D. Ovoshchnikov, R. H. Adnan, D. Appadoo, V. Golovko, G. Andersson and G. F. Metha, *RSC Adv.*, 2013, **3**, 22140-22149.

48 T. Bennett, R. H. Adnan, J. F. Alvino, V. Golovko, G. G. Andersson and G. F. Metha, *Inorg. Chem.*, 2014, **53**, 4340-4349.

49 H. Wang, Y. Xie, R. B. King and H. F. Schaefer III, *J. Am. Chem. Soc.*, 2006, **128**, 11376-11384.

50 T. Andruniow, M. Jaworska, P. Lodowski, M. Z. Zgierski, R. Dreos, L. Randaccio and P. M. Kozlowski, *J. Chem. Phys.* 2008, **129**,085101 - 085101-14.

51 M. R. Silva-Junior, M. Schreiber, S. P. A. Sauer and W. Thiel, *J. Chem. Phys.* 2008, **129**,104103 - 104103-14.

52 D. R. Tyler, R. A. Levenson and H. B. Gray, *J. Am. Chem. Soc.*, 1978, **100**, 7888-7893.

53 F. W. Vergeer, P. Matousek, M. Twrie, P. J. Costa, M. J. Calhorda and F. Hartl, *Chem. Eur. J.*, 2004, **10**, 3451-3460.

54 J. P. Lomont, A. J. Shearer, S. C. Nguyen and C. B. Harris, *Organometallics*, 2013, **32**, 2178-2186.

55 Y. Kou, H. Li Wang, M. Te, T. Tanaka and M. Nomura, *J. Catal.*,1993, **141**, 660-670.

56 M. J. Calhorda, P. J. Costa, F. Hartl and F. W. Vergeer, *C. R. Chimie.*, 2005, **8**, 1477-1486.

57 J. R. Norton, J. P. Collman, G. Dolcetti and W. T. Robinson, *Inorg. Chem.*, 1972, **11**(2), 382-388.

58 D. Asturiol and A. Worth, *The use of chemical reactivity Assays in toxycity prediction* E. Farmi 2749, 21027 Ispra(VA), Italy

59 M. Ishihara, M. Kawase, G. Westman, K. Samuelsson, N. Motohashi and H. Sakagami, *Anticancer Research*, 2007, **27**, 4053-4058.

60 G. Gasser, I. Ott and N. Metzler-Nolte, *J. Med. Chem.*, 2011, **54**, 3-25.

61 www.chemosophia.com